Neuro-Oncology Advances
6(1), vdae069, 2024 | https://doi.org/10.1093/noajnl/vdae069 | Advance Access date 8 May 2024

Hemizygous deletion of cyclin-dependent kinase inhibitor 2A/B with p16 immuno-negative and methylthioadenosine phosphorylase retention predicts poor prognosis in IDH-mutant adult glioma

Ryosuke Otsuji, Nobuhiro Hata, Hidetaka Yamamoto, Daisuke Kuga, Ryusuke Hatae, Yuhei Sangatsuda, Yutaka Fujioka, Naoki Noguchi, Aki Sako, Osamu Togao, Tadamasa Yoshitake, Akira Nakamizo, Masahiro Mizoguchi, and Koji Yoshimoto

All author affiliations are listed at the end of the article

Corresponding Author: Nobuhiro Hata, MD, PhD, Department of Neurosurgery, Oita University Faculty of Medicine, 1-1 Idaigaoka, Hasamamachi, Yufu, Oita, 879-5593, Japan (hatanobu66@oita-u.ac.jp).

Abstract

Background. Homozygous deletion of the tumor suppression genes cyclin-dependent kinase inhibitor 2A/B (*CDKN2A/B*) is a strong adverse prognostic factor in IDH-mutant gliomas, particularly astrocytoma. However, the impact of hemizygous deletion of *CDKN2A/B* is unknown. Furthermore, the influence of *CDKN2A/B* status in IDH-mutant and 1p/19q-codeleted oligodendroglioma remains controversial. We examined the impact of *CDKN2A/B* status classification, including hemizygous deletions, on the prognosis of IDH-mutant gliomas.

Methods. We enrolled 101 adults with IDH-mutant glioma between December 2002 and November 2021. *CDKN2A/B* deletion was evaluated with multiplex ligation-dependent probe amplification (MLPA). Immunohistochemical analysis of p16/MTAP and promoter methylation analysis with methylation-specific MLPA was performed for cases with *CDKN2A/B* deletion. Kaplan – Meier plots and Cox proportion hazards model analyses were performed to evaluate the impact on overall (OS) and progression-free survival.

Results. Of 101 cases, 12 and 4 were classified as hemizygous and homozygous deletion, respectively. Immunohistochemistry revealed p16-negative and MTAP retention in cases with hemizygous deletion, whereas homozygous deletions had p16-negative and MTAP loss. In astrocytoma, OS was shorter in the order of homozygous deletion, hemizygous deletion, and copy-neutral groups (median OS: 38.5, 59.5, and 93.1 months, respectively). Multivariate analysis revealed hazard ratios of 9.30 ($P = .0191$) and 2.44 ($P = .0943$) for homozygous and hemizygous deletions, respectively.

Conclusions. *CDKN2A/B* hemizygous deletions exerted a negative impact on OS in astrocytoma. Immunohistochemistry of p16/MTAP can be utilized to validate hemizygous or homozygous deletions in combination with conventional molecular diagnosis.

Key Points

- The impact of *CDKN2A/B* Hemi-del was evaluated in patients with IDH-mutant glioma.
- In astrocytoma, OS was shorter in Hemi-del compared with copy-neutral.
- IHC clearly detected Hemi-del with p16-negative and MTAP retention.

Importance of the Study

Homozygous deletion (Homo-del) of cyclin-dependent kinase inhibitor 2A/B (*CDKN2A/B*) is a strong adverse prognostic factor in IDH-mutant gliomas, particularly astrocytoma. However, the impact of hemizygous deletion (Hemi-del) of *CDKN2A/B* is unknown. Furthermore, the influence of *CDKN2A/B* status in IDH-mutant and 1p/19q-codeleted oligodendroglioma is controversial. We evaluated *CDKN2A/B* status in patients with IDH-mutant glioma, using multiplex ligation-dependent probe amplification copy number analysis corrected with IDH-mutant variant allele frequency assessed through digital PCR. In astrocytoma, overall survival (OS) in Hemi-del was between that of Homo-del and copy-neutral. Furthermore, we report the utility of immunohistochemistry (IHC) of p16 and MTAP to distinguish Hemi-del from Homo-del and copy-neutral. We hypothesize that *CDKN2A/B* Hemi-del exerts a negative impact on OS in astrocytoma, and that the unexpensive method of IHC of p16/MTAP can be used to clearly identify Hemi-del.

Adult-type diffuse gliomas are among the most common primary brain tumors,[1] and their molecular characterization is crucial for diagnosis and treatment.[2,3] The homozygous deletion (Homo-del) of cyclin-dependent kinase inhibitor 2A/B (*CDKN2A/B*) is a strong adverse prognostic factor in IDH-mutant gliomas.[4–9] Astrocytoma, IDH-mutant (hereafter astrocytoma) is stratified according to the 2021 WHO classification of CNS tumors into grades 2, 3, or 4, depending on the presence or absence of a *CDKN2A/B* Homo-del.[3]

Previous studies have reported that the chromosome region 9p21, containing the loci encoding $p16^{INK4A}$, $p14^{ARF}$, and $p15^{INK4B}$, is involved in hemizygous deletion (Hemi-del) and Homo-del in gliomas.[10–12] *CDKN2A* encodes $p16^{INK4a}$ and $p14^{ARF}$ by alternative splicing and distinction of reading frames, while *CDKN2B* exists in their vicinity to encode $p15^{INK4b}$. *CDKN2A/B* are tumor suppression genes; $p16^{INK4A}$ and $p15^{INK4B}$ induce a G1 cell cycle arrest by inhibiting the activity of cyclin-dependent kinases 4 and 6 (CDK4 and CDK6) from phosphorylating the RB protein,[13–15] while $p14^{ARF}$ activates p53[14,15] by binding to and promoting the rapid degradation of MDM2.[16] Based on Knudson's 2-hit hypothesis, oncogenesis may be induced by a second hit of methylation or mutation in the counter allele without deletion of tumor suppression genes.[17] *CDKN2A* promoter methylation occurs frequently, especially in lower-grade gliomas,[18–20] and cases with Hemi-del *CDKN2A/B* accompanied by promoter methylation may, theoretically, present similar to Homo-del of *CDKN2A/B*.

Although Homo-del of *CDKN2A/B* is a definitive prognostic factor, the clinical significance of Hemi-del is unclear. Recent studies on the prognostic implications of CDKN2A/B Hemi-del show that it may adversely affect the prognosis of lower-grade gliomas.[21,22] However, there is still no consensus on this matter. Furthermore, the influence of *CDKN2A/B* status in oligodendroglioma, IDH-mutant, and 1p/19q-codeleted (hereafter oligodendroglioma) remains controversial.[5,23–26]

We evaluated the prognosis of IDH-mutant glioma cases with Hemi-del *CDKN2A/B*. Furthermore, we performed external verification using The Cancer Genome Atlas (TCGA)-LGG public dataset[23] to validate our results. We also examined the promoter methylations of *CDKN2A/B,* the 2-hit hypothesis for *CDKN2A/B,* and the potential usefulness of immunohistochemical analyses.

Materials and Methods

Patients

We enrolled 101 patients (> 18 years old) with newly diagnosed IDH-mutant glioma between December 2002 and November 2021 (Supplementary Figure S1). The sample size was not statistically determined prior to the study. The molecular features of all patients were confirmed as described below. All patients received an integrated diagnosis using the WHO 2021 classification based on histopathology and molecular diagnosis. Oligodendroglioma was defined as satisfying both IDH-mutant and chromosome 1p/19q codeletion. One case of IDH-mutant and *TERT* promoter mutations without 1p/19q codeletion was excluded. The clinical characteristics of the patients are summarized in Table 1. At our facility, the policy for adjuvant treatment was as follows: post-treatment was not performed for grade 2 astrocytoma when complete resection was achieved, while chemotherapy with nimustine (ACNU) and radiotherapy (RT) were performed when less than subtotal resection was achieved. For grade 3, ACNU and RT were performed regardless of the degree of resection.[27] For grade 4, synchronous RT with temozolomide was performed, similar to glioblastoma. For oligodendroglioma, only chemotherapy with ACNU was performed, and RT was deferred as much as possible.[28,29] This study was approved by the Kyushu University Institutional Review Board for Clinical Research (848 – 00) and conducted in accordance with the 1964 Declaration of Helsinki (as revised in October 2013). Informed consent was obtained from all patients.

Molecular Diagnosis

DNA was extracted from intraoperative snap-frozen tumor samples using a QIAamp DNA mini kit (Qiagen Science, Germantown, Maryland, USA). Hotspot mutations of *IDH1, IDH2, BRAF*, and *H3F3A* were confirmed by Sanger sequencing following high-resolution melt analysis.[30–34] *TERT* promoter mutations were assessed with Sanger sequencing.[30,32,33,35] *MGMT* methylation status was evaluated using methylation-specific PCR.[30,32,36] Copy number alterations were detected by multiplex ligation-dependent

Table 1. Clinical and Molecular Features (n = 101)

Variable assessed	All (n = 101)	Astrocytoma, IDH-mutant (n = 52)	Oligodendroglioma, IDH-mutant and 1p/19q-codeleted (n = 49)
Age, median (range)	41 (19 – 78)	34.5 (19 – 71)	47 (20 – 78)
≤50 (%)	28 (27.7)	44 (84.6)	29 (59.2)
>50 (%)	73 (72.3)	8 (15.4)	20 (40.8)
Male sex (%)	59 (58.4)	34 (63.0)	26 (53.1)
Tumor size (mm), median (range)	55 (22 – 144)	55 (22 – 144)	50 (25 – 92)
KPS			
median (range)	90 (50 – 100)	90 (50 – 100)	90 (60 – 100)
>80 (%)	87 (86.1)	44 (84.6)	43 (87.8)
≤80 (%)	14 (13.9)	8 (15.4)	6 (12.2)
EOR			
>90% (%)	61 (60.4)	28 (53.8)	33 (67.3)
≤90% (%)	40 (39.6)	24 (46.2)	16 (32.7)
Radiation therapy (%)			
(+)	34 (33.7)	33 (63.5)	1 (2.0)
(–)	67 (66.3)	19 (36.5)	48 (98.0)
Chemotherapy (%)			
(+)	82 (80.4)	36 (69.2)	45 (91.8)
(–)	20 (19.6)	16 (30.8)	4 (8.2)
WHO grade (%)			
2	54 (53.9)	28 (53.8)	26 (53.1)
3	44 (43.1)	21 (40.4)	23 (46.9)
4	3 (2.9)	3 (5.8)	—
IDH-mutant (%)	101 (100)	52 (100)	49 (100)
p*TERT* mutant (%)	49 (48.5)	0 (0)	49 (100)
1p/19q codeletion (%)	49 (48.5)	0 (0)	49 (100)
CDKN2A/B copy number (%)			
Homozygous deletion	4 (4.0)	3 (5.8)	1 (2.0)
Hemizygous deletion	12 (11.9)	9 (17.3)	3 (6.1)
Copy-neutral	85 (84.2)	40 (76.9)	45 (91.8)

CDKN2A/B, cyclin-dependent kinase inhibitor 2A/B; EOR, extent of resection; IDH, isocitrate dehydrogenase; KPS, Karnofsky Performance Scale; p*TERT,* promoter of telomerase reverse transcriptase; WHO, World Health Organization.

probe amplification (MLPA) with P088-D1 and P105-D3 probe sets (MRC-Holland, Amsterdam, Netherlands). Following the MLPA reaction, DNA fragment analysis was performed using a 3730 DNA analyzer (Applied Biosystems, Waltham, MA, USA) and analyzed with Coffalyser® software (MRC-Holland).[30,37] The 1p/19q status was confirmed by loss of heterozygosity analysis using PCR-based microsatellite markers,[32,38–41] and MLPA with P088-D1 probemix. *CDKN2A/B* deletion was analyzed with both P088-D1 and P105-D3 kits, and other copy number alterations, including those for *EGFR*, *PTEN*, *PDGFRA*, *CDK4*, and *TP53* were confirmed using P105-D3. The thresholds of 0.8 and 1.2 were set for the detection of deletions and gains.[30,42] However, since the copy number analysis of MLPA is based on relative quantification, it is affected by the tumor content rate. Therefore, for *CDKN2A/B* deletion, we set custom thresholds for each case using the following formula (eg, for a tumor content of 80%, the thresholds for Hemi-del and Homo-del were 0.8 and 0.4, respectively).

Tumor cell rate = IDH-mutant VAF × 2
Hemi-del cutoff = 1 – Tumor cell rate × 0.25
Homo-del cutoff = 1 – Tumor cell rate × 0.75

Details of how to derive the formula are described in Supplementary Methods. For the tumor content rate, we used the IDH-mutant variant allele frequency (VAF) from the digital PCR. We also confirmed that the 1p and 19q copy numbers were Hemi-del in oligodendroglioma. *CDKN2A/B* promoter methylation was assessed using methylation-specific MLPA (MS-MLPA) with ME024-B3 probemix (MRC-Holland), according to the manufacturer's protocol. Aberrant methylation was identified by the appearance of

a signal peak after HhaI enzyme digestion, and methylation was scored when the calculated ratio compared with normal unmethylated loci was more than 15%.[43]

Digital PCR

Since copy number analysis using MLPA is affected by dilution with genomic DNA derived from non-tumor cells; the ratio of IDH-mutant to IDH-wild type was confirmed by digital PCR using the QuantStudio™ 3D Digital PCR System (ThermoFisher Scientific, Waltham, MA, USA) or QuantStudio™ Absolute Q™ digital PCR system (ThermoFisher Scientific) to confirm the IDH-mutant VAF. Diluted DNA samples (3.3 ng/μL) were used to perform PCR with a custom-made assay (Assay ID: ANDJ4XD, Life Technologies, Carlsbad, CA, USA) for detecting IDH-wild type and IDH-mutant alleles.[37,44] VAF of the IDH-mutant was calculated as the ratio of the number of IDH-mutant wells to that of wells containing IDH-mutant and/or IDH-wild type signals, and was analyzed using QuantStudio™ 3D Analysis Suite™ (version 3.1.6-PRC-build18) or QuantStudio™ AbsoluteQ™ Digital PCR Software v6.2.1.

Immunohistochemical Analyses

Specimens were fixed in 10% formalin, gradient-dehydrated with ethanol, and immersed in paraffin. Serial 4-μm-thick sections were cut from the formalin-fixed, paraffin-embedded (FFPE) tissue blocks, and immunohistochemical staining for p16 and methylthioadenosine phosphorylase (MTAP) was performed. Primary antibodies for p16 (mouse monoclonal, E6H4, prediluted, Roche, Heidelberg, Germany) and MTAP (mouse monoclonal, 42-T, × 100, Santa Cruz Biotechnology, Dallas, TX, USA) were used. Pretreatment for heat-induced epitope retrieval was conducted with EDTA-based CC1 buffer (Roche) for p16 and ER2 buffer (Roche) for MTAP. After pretreatment, the primary antibodies were mounted on the tissue sections, and subsequent reactions were conducted with an ultraView universal DAB detection kit (Roche) on a fully automated immunohistochemical staining system (Benchmark ULTRA; Ventana Medical Systems, Tuscan, AZ, USA).

P16 protein expression was classified using a 4-step scale: 0: < 1%, 1: 1% to < 10%, 2: 10% to < 50%, 3: 50% or more. In this study, scales 0 and 1 were evaluated as negative, whereas 2 and 3 were positive. HPV-positive oropharyngeal carcinoma was used as an external control.[45] MTAP protein expression was defined as retained if almost all tumor cells and endothelial cells (internal control) exhibited positive staining. If almost all tumor cells demonstrated no immunoreactivity for MTAP with positive staining in endothelial cells, the case was defined as a loss. Immunohistochemical evaluation of p16 and MTAP using direct light microscopy was performed by an experienced pathologist (HY) who was blinded to the molecular features.

Fluorescence In Situ Hybridization for *CDKN2A/B* deletion

As a supplementary experiment, fluorescence in situ hybridization (FISH) was performed for case 11, in which heterogeneity within the tumor was found. FISH was performed on FFPE sections using the p16/CEN9q Dual Color FISH Probe (Product No. GC002, GSP Lab, Inc., Kanagawa, Japan) to assess the *CDKN2A/B* copy number. Green and red signals were identical to FITC-labeled CEN9q and Texas-red-stained p16, respectively. FISH signals were evaluated in at least 50 tumor cell nuclei. If green (CEN9q)-only signal patterns with loss of 2 red (p16) signals were observed in > 30% of the cells, the case was defined as Homo-del of *CDKN2A/B*. If the FISH results did not meet the criteria of Homo-del and the loss of one red (p16) signal pattern was observed in > 30% of the cells, the case was defined as Hemi-del of *CDKN2A/B*.

The Cancer Genome Atlas dataset

To validate our results, an additional validation cohort from a public dataset from the TCGA-LGG project was analyzed.[26] DNA copy numbers and IDH status were retrieved from the publicly available UCSC Xena site (http://xena.ucsc.edu/). Clinical data including survival data were obtained from the NCI Cancer Genomic Data Commons (NCI-GDC: https://gdc.cancer.gov). Of the 538 cases in the dataset, the copy number analysis was unavailable in 11, 5 were without survival data, and 122 cases with IDH-wild type (96 cases) or unknown (26 cases) were excluded. Finally, 400 cases were analyzed. The 1p/19q codeletion was evaluated: 261 cases without the codeletion were classified as astrocytomas, while 139 cases with the codeletion were classified as oligodendrogliomas. Homo-del or Hemi-del *CDKN2A/B* was defined based on the copy number output generated by the GISTIC 2.0 pipeline.[46] Methylation status was evaluated using beta-value, and stratified as hypermethylated (beta > 0.5) or unmethylated (beta ≤ 0.5).

Statistical Analysis

All statistical analyses were performed using JMP Pro version 16.0.0 (SAS Institute Inc., Cary, NC, USA). The distribution of VAF was confirmed by histograms, and outliers were confirmed based on the median and quartiles. Kaplan – Meier analysis was conducted to evaluate overall (OS) and progression-free survival (PFS). The log-rank test was used to compare survival distributions. Univariate and multivariate Cox proportion hazards model analyses were performed to evaluate hazard ratios (HRs) and 95% confidence intervals (CIs) for *CDKN2A/B* status and other putative prognostic factors. Factors for multivariate analysis included variables with significant or trending differences in univariate analyses or those previously reported to have significant differences. *P* values were calculated using 2-tailed tests. Statistical significance was set at $P < .05$.

Results

Evaluation of *CDKN2A/B* Status and Immunohistochemical Analysis

Copy number analysis using MLPA detected a *CDKN2A/B* deletion in 16 out of 101 cases. Of those, 12 were astrocytoma and 4 were oligodendroglioma. Based on

Table 2. Case With *CDKN2A/B* Copy Number Alteration (n = 16)

Case	Integrated diagnosis (grade)	Pathological diagnosis		Molecular diagnosis							
		Histology	p16 (score)	MTAP	***IDH1*** (VAF, %)	1p/19q codel	p***TERT***	***CDKN2A/B*** status	***CDKN2A*** methylation (M/U)	Others
1	Astrocytoma, IDH-mut. (4)	AA	Negative (0)	Loss	R132H (47.0)	–	Wt	Homo	—	
2	Astrocytoma, IDH-mut. (4) [b]	DA	Negative (0)	Loss	R132H (22.9)	–	Wt	Homo	—	*TP53* hemi
3	Astrocytoma, IDH-mut. (4)	OD	N/A	N/A	R132H (49.1)	–	Wt	Homo	—	*EGFR* gain, *CDK4* gain
4	Astrocytoma, IDH-mut. (3)	AA	Negative (0)	Retain	R132H (43.4)	–	Wt	Hemi	M	
5	Astrocytoma, IDH-mut. (3)	AA	Negative (1)	Retain	R132H (36.7)	–	Wt	Hemi	M	*EGFR* gain
6	Astrocytoma, IDH-mut. (3)	AA	Negative (1)	Retain	R132H (42.3)	–	Wt	Hemi	U	*PDGFRA* amp
7	Astrocytoma, IDH-mut. (3)	AA	Negative (1)	Retain	R132H (42.8)	–	Wt	Hemi	U	
8	Astrocytoma, IDH-mut. (2)	OA	Negative (1)	Retain	R132H (28.5)	–	Wt	Hemi	U	*TP53* hemi
9	Astrocytoma, IDH-mut. (2)	OA	Negative (0)	Retain	R132H (41.5)	–	Wt	Hemi	M	*TP53* hemi
10	Astrocytoma, IDH-mut. (2)	DA	Negative (1)	Retain	R132H (44.5)	–	Wt	Hemi	M	
11	Astrocytoma, IDH-mut. (2)	DA	Negative† (1†)	Retain	R132H (40.5)	–	Wt	Hemi	M	
12	Astrocytoma, IDH-mut. (2)	DA	Negative (1)	Retain	R132H (52.0)	–	Wt	Hemi	M	*TP53* homo
13	Oligodendroglioma, IDH-mut. (3)	AO	Negative (0)	Loss	R132H (32.7)	+	C228T	Homo	—	
14	Oligodendroglioma, IDH-mut. (3)	AO	N/A	N/A	R132H (44.0)	+	C250T	Hemi	M	*EGFR* gain
15	Oligodendroglioma, IDH-mut. (3)	AO	Negative (1)	Retain	R132H (57.8)	+	C228T	Hemi	U	*EGFR* gain, *TP53* hemi
16	Oligodendroglioma, IDH-mut. (3)	AOA	Negative (1)	Retain	R132H (47.6)	+	C228T	Hemi	M	*TP53* hemi

AA, anaplastic astrocytoma; amp, amplification; AO, anaplastic oligodendroglioma; AOA, anaplastic oligoastrocytoma; *CDK4*, cyclin-dependent kinase 4; *CDKN2A/B*, cyclin-dependent kinase inhibitor 2A/B; codel, codeletion; DA, diffuse astrocytoma; *EGFR*, epidermal growth factor receptor; Hemi, hemizygous deletion; Homo, homozygous deletion; IDH, isocitrate dehydrogenase; mut, mutant; N/A, not available; OA, oligoastrocytoma; p*TERT*, promoter of telomerase reverse transcriptase; *TP53*, tumor protein P53; VAF, valiant allele frequency; Wt, wild type.
†Heterogeneity within the tumor was found. p16-positive (score 3) and p16-negative (score 1) cells were coexisting. The score of the region with the lowest expression was adopted for the p16 status.

MLPA results, 2 Homo-del and 10 Hemi-del cases of *CDKN2A/B* were identified in the astrocytomas, whereas 1 Homo-del and 3 Hemi-del cases were found in the oligodendrogliomas (Tables 1 and 2). MS-MLPA was performed on 12 cases with Hemi-del in MLPA to evaluate the *CDKN2A/B* promoter methylation. *CDKN2A* promoter methylation was observed in 8 of the 12 cases (Table 2 and Supplementary Figure S2).

Immunohistochemical analysis of p16/MTAP was performed on 16 cases with *CDKN2A/B* deletion. The results and representative cases are presented in Table 2 and Figure 1, respectively. Immunohistochemical staining revealed both p16/MTAP loss in the Homo-del cases, whereas p16 was lost and MTAP was retained in the Hemi-del cases (Figure 1C). In case 11, heterogeneity with different immunohistochemical results was observed within the tumor tissue, suggesting a cluster of copy-neutral (Neutral) and Hemi-del populations (Table 2 and Supplementary Figure S3). The supplementary FISH evaluation revealed clusters of Neutral and Hemi-del cells, supporting the results of immunohistochemistry.

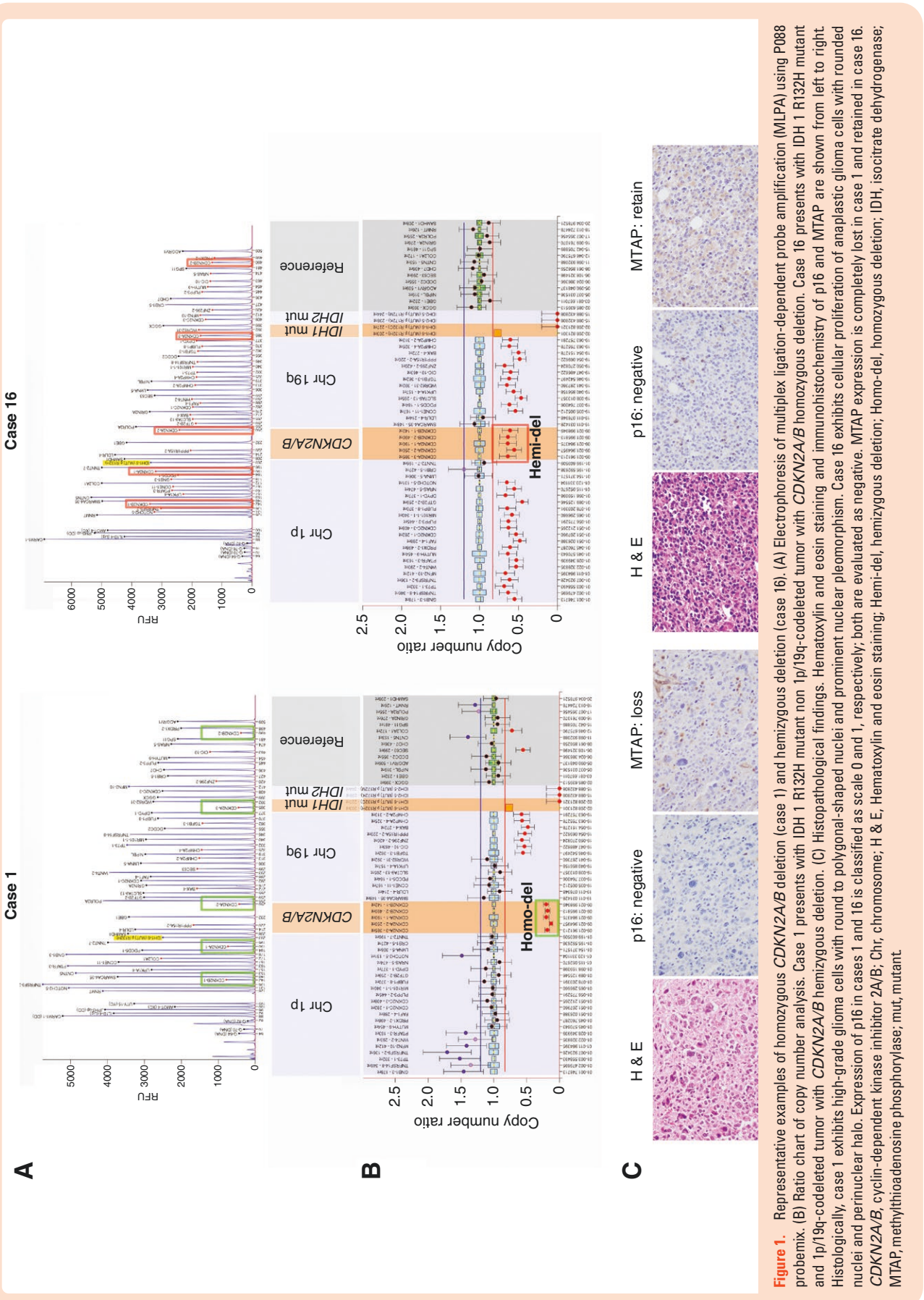

Figure 1. Representative examples of homozygous *CDKN2A/B* deletion (case 1) and hemizygous deletion (case 16). (A) Electrophoresis of multiplex ligation-dependent probe amplification (MLPA) using P088 probemix. (B) Ratio chart of copy number analysis. Case 1 presents with IDH 1 R132H mutant non 1p/19q-codeleted tumor with *CDKN2A/B* homozygous deletion. Case 16 presents with IDH 1 R132H mutant and 1p/19q-codeleted tumor with *CDKN2A/B* hemizygous deletion. (C) Histopathological findings. Hematoxylin and eosin staining and immunohistochemistry of p16 and MTAP are shown from left to right. Histologically, case 1 exhibits high-grade glioma cells with round to polygonal-shaped nuclei and prominent nuclear pleomorphism. Case 16 exhibits cellular proliferation of anaplastic glioma cells with rounded nuclei and perinuclear halo. Expression of p16 in cases 1 and 16 is classified as scale 0 and 1, respectively; both are evaluated as negative. MTAP expression is completely lost in case 1 and retained in case 16. *CDKN2A/B*, cyclin-dependent kinase inhibitor 2A/B; Chr, chromosome; H & E, Hematoxylin and eosin staining; Hemi-del, hemizygous deletion; Homo-del, homozygous deletion; IDH, isocitrate dehydrogenase; MTAP, methylthioadenosine phosphorylase; mut, mutant.

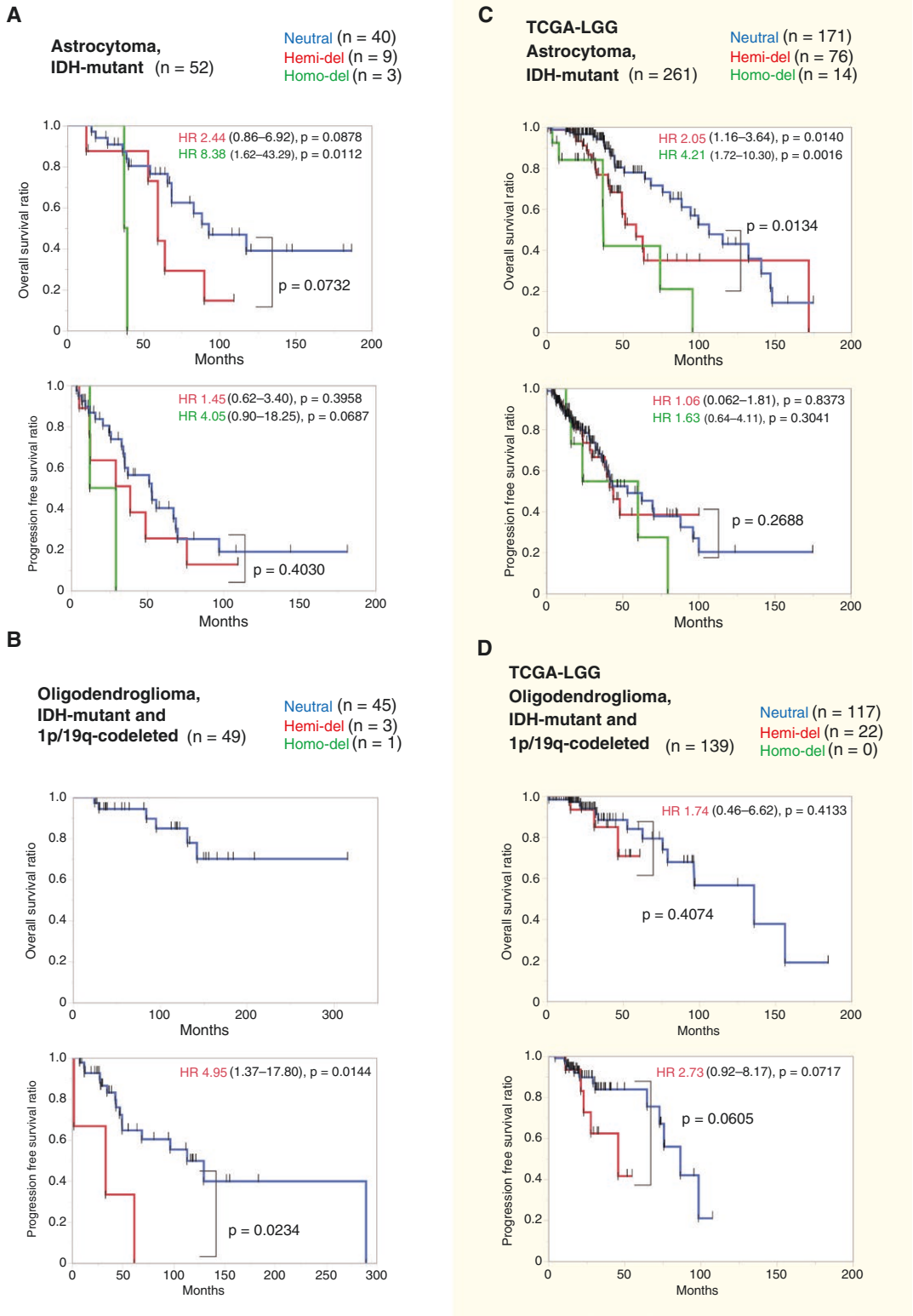

Figure 2. Kaplan–Meier plots of astrocytoma and oligodendroglioma stratified by *CDKN2A/B* status. A: IDH-mutant astrocytoma cases in our cohort. The duration of OS increased in the order of Homo-del, Hemi-del, and Neutral groups (median OS: 38.5, 59.5, and 93.1 months, respectively). OS was shorter for Hemi-del than for Neutral ($P = .0732$). B: IDH-mutant and 1p/19q-codeleted oligodendroglioma in our cohort. Hemi-del had a significantly shorter PFS than Neutral (median 33.3 and 113.6 months, respectively, $P = .0234$). C: IDH-mutant astrocytoma in The Cancer Genome Atlas (TCGA)-LGG data. In this cohort, Hemi-del and Neutral differed significantly ($P = .0134$). D: IDH-mutant and 1p/19q-codeleted oligodendroglioma in TCGA-LGG data. There was no significant difference in PFS between Hemi-del and Neutral (45.8 and 86.7 months, respectively, $P = .0605$). Hemi-del, hemizygous deletion of *CDKN2A/B*; Homo-del, homozygous deletion of *CDKN2A/B*; HR, hazard ratio; OS, overall survival; PFS, progression-free survival; Neutral, copy-neutral.

Table 3. Clinical and Molecular Prognostic Factors

Variable assessed	Astrocytoma, IDH-mutant (*n* = 52) Case (%)	OS				PFS			
		Univariate analysis		Multivariate analysis		Univariate analysis		Multivariate analysis	
		HR (95% CI)	*P* value	HR (95% CI)	*P* value	HR (95% CI)	*P* value	HR (95% CI)	*P* value
Age > 50	8 (15.4)	1.05 (0.24 – 4.53)	.9455	1.55 (0.34 – 7.02)	.5674	1.38 (0.48 – 3.97)	.5539	1.74 (0.57 – 5.32)	.3330
Male sex	34 (63.0)	1.01 (0.39 – 2.60)	.9788	—	—	1.09 (0.50 – 2.37)	.8362	—	—
KPS ≤ 80	8 (15.4)	1.97 (0.65 – 5.96)	.2297	0.80 (0.20 – 3.20)	.7533	0.99 (0.38 – 2.59)	.9810	0.61 (0.20 – 1.91)	.4000
EOR ≤ 90%	24 (46.2)	1.94 (0.82 – 4.59)	.1298	1.96 (0.76 – 5.05)	.1657	1.42 (0.69 – 2.90)	.3397	1.66 (0.75 – 3.68)	.2158
Radiation therapy (-)	19 (36.5)	0.63 (0.25 – 1.63)	.3455	—	—	1.35 (0.61 – 3.01)	.4629	—	—
Chemo-therapy (-)	16 (30.8)	0.50 (0.17 – 1.51)	.2203	—	—	1.11 (0.47 – 2.62)	.8169	—	—
WHO grade									
2	28 (53.8)	Ref	—	—	—	Ref	—	—	—
3	21 (40.4)	0.89 (0.35 – 2.24)	.7989.			0.56 (0.26 – 1.19)	.1332.		
4	3 (5.8)	5.09 (1.03 – 25.21)	0462			3.23 (0.71 – 14.80)	1303		
CDKN2A/B status									
Copy-neutral	40 (76.9)	Ref	—	Ref	—	Ref	—	Ref	—
Hemizygous deletion	9 (17.3)	2.34 (0.88 – 6.20)	.0878	2.44 (0.86 – 6.92)	0.0943	1.45 (0.62 – 3.40)	.3958	1.54 (0.65 – 3.70)	0.3288
Homozygous deletion	3 (5.8)	8.38 (1.62 – 43.29)	.0112	9.30 (1.44 – 60.04)	0.0191	4.05 (0.90 – 18.25)	.0687	5.36 (1.01 – 28.41)	0.0487

Variable assessed	Oligodendro-glioma, IDH-mutant and 1p/19q-codeleted (n = 49) Case (%)	OS†		PFS			
		Univariate analysis		Univariate analysis		Multivariate analysis	
		HR (95% CI)	*P* value	HR (95% CI)	*P* value	HR (95% CI)	*P* value
Age > 50	20 (40.8)	2.73 (0.51 – 14.61)	.2415	1.40 (0.53 – 3.65)	.4963	0.99 (0.33 – 2.93)	.9861
Male sex	26 (53.1)	0.82 (0.16 – 4.15)	.8111	1.27 (0.50 – 3.23)	.6095	—	—
KPS ≤ 80	6 (12.2)	1.84 (0.21 – 15.79)	.5772	0.94 (0.22 – 4.12)	.9363	0.37 (0.07 – 2.05)	.2562
EOR ≤ 90%	16 (32.7)	2.73 (0.49 – 15.22)	.2530	1.85 (0.73 – 4.70)	.1945	2.81 (0.96 – 8.26)	.0602
Radiation therapy (-)	48 (98.0)	N/A	N/A	N/A	N/A	—	—
Chemotherapy (-)	4 (8.2)	N/A	N/A	0.41(0.05 – 3.09)	.3860	—	—
WHO grade							
2	26 (53.1)	Ref	—	Ref	—	—	—
3	23 (46.9)	0.61 (0.11 – 3.34)	.5685	1.43 (0.56 – 3.63)	.4542		
CDKN2A/B status							
Copy-neutral	45 (91.8)	Ref	—	Ref	—	Ref	—
Hemizygous deletion	3 (6.1)	N/A	N/A	4.95 (1.37 – 17.80)	.0144	7.43 (1.58 – 34.98)	.0112
Homozygous deletion	1 (2.0)	N/A	N/A	N/A	N/A	N/A	N/A

CDKN2A/B, cyclin-dependent kinase inhibitor 2A/B; CI, confident interval; EOR, extent of resection; HR, hazard ratio; IDH, isocitrate dehydrogenase; KPS, Karnofsky Performance Scale; N/A, not available (the factor could not be analyzed because of unreached endpoint); OS, overall survival; PFS, progression-free survival; Ref, reference; WHO, World Health Organization.

†Only univariate analysis was performed in oligodendrogliomas because analysis of *CDKN2A/B* hemi/homozygous deletion was unable because of unreached endpoint.

Impact of *CDKN2A/B* Status on Survival Outcomes

OS and PFS were analyzed by dividing the cases into 3 groups based on *CDKN2A/B* status: Homo-del, Hemi-del, and Neutral. Kaplan – Meier plots are presented in Figures 2A and B. In astrocytoma, OS was shorter in the order of Homo-del, Hemi-del, and Neutral groups, with a median OS of 37.5, 59.5, and 93.1 months, respectively. Hemi-del tended to have a shorter OS than Neutral ($P = .0732$). In oligodendroglioma, OS could not be compared because one Homo-del and 3 Hemi-del cases did not reach the endpoint. Regarding PFS, in astrocytoma, the time-to-recurrence tended to be shorter in the order of Homo-del, Hemi-del, and Neutral, with median PFS of 20.9, 38.9, and 53.0 months, respectively. There was no significant difference in PFS between Hemi-del and Neutral in astrocytoma ($P = .4030$). In oligodendroglioma, Hemi-del and Neutral were compared because one Homo-del case did not reach the endpoint. The recurrence period was significantly shorter in the Hemi-del than in the Neutral group, with median PFS of 33.3 and 113.6 months, respectively ($P = .0234$).

The results of Cox proportional hazards model analysis are presented in Table 3. In univariate Cox proportional hazards model for OS for astrocytoma, compared to Neutral, Homo-del, and Hemi-del exhibited HRs of 8.38 (95% CI: 1.62 – 43.29, $P = .0112$) and 2.33 (95% CI: 0.88 – 6.20, $P = .0878$), respectively. Multivariate analysis revealed similar results (Homo-del HR: 9.30, 95% CI: 1.44 – 60.04, $P = .0191$; Hemi-del HR: 2.44, 95% CI: 0.86 – 6.92, $P = .0943$). No other factors were significant in the multivariate analysis. Regarding PFS for oligodendrogliomas, Hemi-del had HRs of 4.95 (95% CI: 1.37 – 17.80, $P = .0144$) and 7.43 (95% CI: 1.58 – 34.98, $P = .0112$) in univariate and multivariate analysis, respectively.

Correlation Between *CDKN2A/B* Status and Malignant Transformation in Astrocytomas

We evaluated potential differences in malignant transformation according to *CDKN2A/B* status in astrocytoma. Of the 52 cases of astrocytoma, 31 recurred during follow-up. Of those, we extracted twenty cases in which surgical resection was performed after recurrence, and evaluated their corresponding pathological findings. Malignant transformation was defined as changes in the histopathological features of a "glioblastoma" according to the WHO 2016 classification, including necrosis and microvascular proliferation. Malignant transformation was confirmed in 1 of the 1 Homo-del, 2 of the 3 Hemi-del, and 5 of the 16 Neutral patients. The time from initial surgery to recurrence with malignant transformation was shortest in Homo-del and longest in Neutral. The median was 26.3 months for Homo-del, 49.0 months for Hemi-del, and not reached for Neutral (Supplementary Figure S4). No significant difference was observed between Hemi-del and Neutral; however, Hemi-del tended to require less time for malignant transformation than Neutral ($P = .1112$).

TCGA Cohort

For external validation, OS was evaluated based on the *CDKN2A/B* status of Homo-del, Hemi-del, and Neutral using the TCGA cohort. The allocation results for each group are presented in Supplementary Table S1. Kaplan – Meier plots are presented in Figure 2C and D. Astrocytoma cases exhibited significantly shorter OS in the order of Homo-del, Hemi-del, and Neutral (median OS: 37.3, 58.7, and 106.7 months, respectively; Figure 2C). Hemi-del and Neutral differed significantly ($P = .0134$). The HRs were 2.05 (95% CI: 1.16 – 3.64, $P = .0140$) and 4.21 (95% CI: 1.72 – 10.30, $P = .0016$) for Hemi-del and Homo-del, respectively, with Neutral as a reference. Hemi-del had an intermediate risk between Neutral and Homo-del. The median PFS time for Homo-del, Hemi-del, and Neutral was 60.3, 44.1, and 53.5 months, respectively, with no difference among the groups. Similarly, the effect of *CDKN2A/B* status was not significant in the Cox proportional hazards model, with HRs of 1.06 (95% CI: 0.62 – 1.81, $P = .8373$) and 1.63 (95% CI: 0.64 – 4.11, $P = .3041$) for Hemi-del and Homo-del, respectively.

In oligodendroglioma cases, no Homo-del were identified, and 19 out of 22 cases of Hemi-del did not reach the endpoint. Therefore, we were unable to compare survival outcomes according to *CDKN2A/B*. There was no significant difference in PFS between Hemi-del and Neutral (median: 45.8 and 86.7 months, respectively, $P = .0605$; Figure 2D). Hemi-del had an HR of 2.73 (95% CI: 0.92 – 8.17, $P = .0717$). In addition, we obtained the copy number of MTAP and methylation array data of *CDKN2A/B* and MTAP to consider the immunohistochemistry results as a supplement. The relationship between *CDKN2A* and *MTAP* deletions (Supplementary Figure S5) and methylation of *CDKN2B, CDKN2A*, and *MTAP* transcription start sites (Figure 3) are presented.

Discussion

We investigated the impact of Hemi-del *CDKN2A/B* on the prognosis of IDH-mutant glioma. In our cohort, OS tended to be shorter for Hemi-del of *CDKN2A/B* in astrocytoma than for Neutral. Also, Hemi-del exhibited an intermediate prognosis between Neutral and Homo-del (Figure 2A). Multivariate analysis suggested that Hemi-del was a negative prognostic factor for OS (Table 3). However, only 9 cases (17.3%) of astrocytoma in our cohort were classified as Hemi-del; therefore, a highly reliable multivariate analysis could not be performed. Whether Hemi-del truly affects the prognosis of astrocytomas needs to be validated with a larger sample size. Thus, an external validation with TCGA-LGG was performed, which revealed that OS was significantly shorter for Hemi-del than for Neutral (Figure 2C). A recent report, in which a survival analysis of Hemi-del *CDKN2A/B* in IDH-mutant astrocytoma was performed, found a similar negative impact on OS, supporting our results.[21,22] These results suggest that the Hemi-del *CDKN2A/B* may have a poorer prognosis than the Neutral. However, there was no significant difference between Hemi-del and Neutral in both our cohort and the TCGA-LGG cohort regarding their impact on recurrence. When comparing the Kaplan–Meier curves of OS and PFS, the survival period after recurrence was longest in the Neutral status, suggesting that the recurrence pattern could be different. Therefore, we evaluated the time for

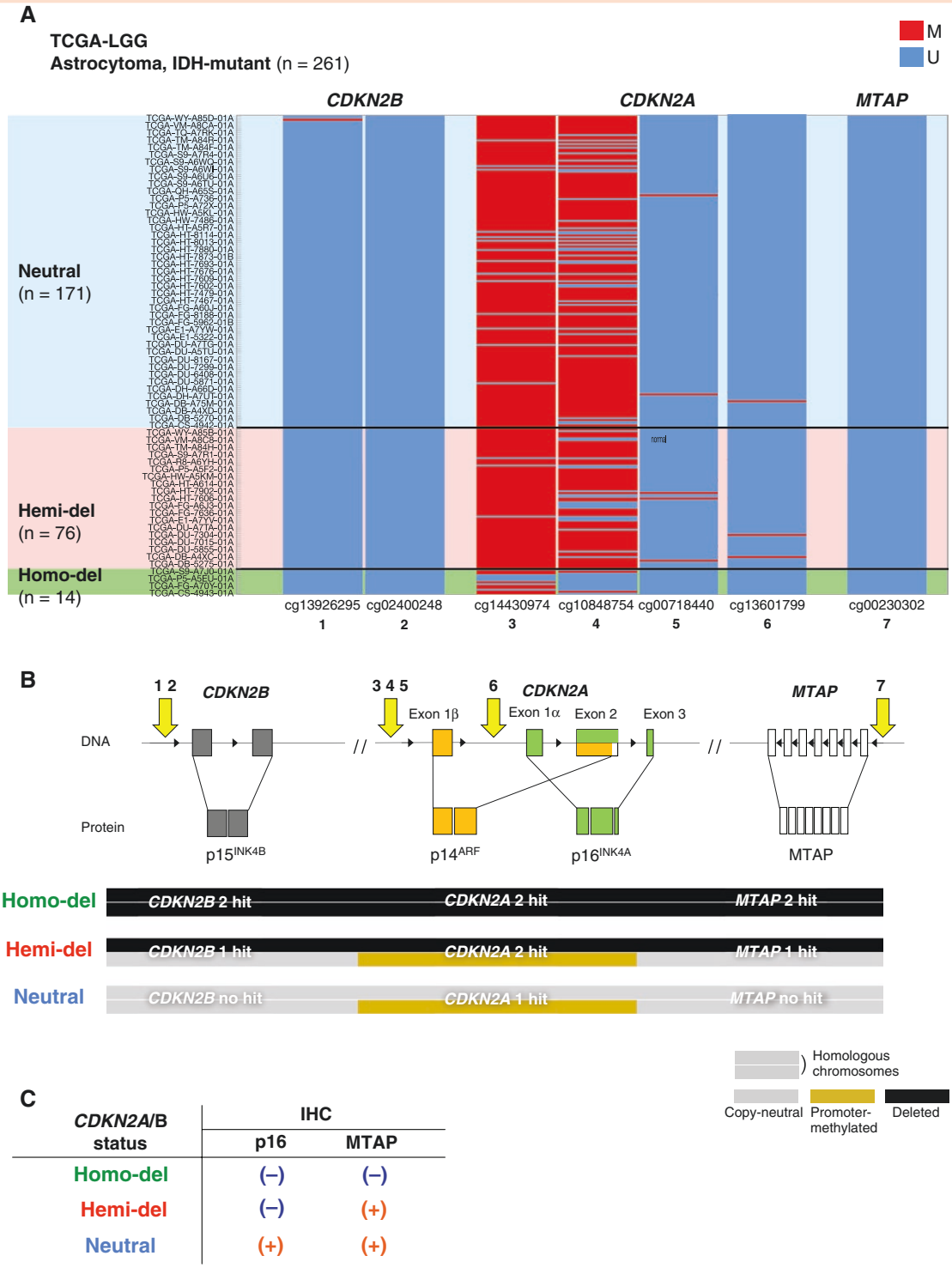

Figure 3. Schematic diagram of *CDKNA2A/B* and *MTAP* loci and heatmap showing the methylation status of transcription start sites. (A) Heatmap showing methylation of the transcription start sites at *CDKNA2B*, *CDKN2A*, and *MTAP* loci in cases of The Cancer Genome Atlas-LGG. Cases are aligned by copy number of *CDKN2A*. *CDKN2B* and *MTAP* are unmethylated, whereas *CDKN2A* has upstream methylations. (B) Schema presents *CDKNA2B*, *CDKN2A*, and *MTAP* loci. The transcription start sites at each locus targeted by the methylation array probes are numbered 1 to 7. The HhaI target of MLPA ME 024 corresponds to *CDKN2B* (1 – 2) and *CDKN2A* (3 – 6). In Homo-del, *CDKN2A/B* and *MTAP* are deleted in both alleles. In Hemi-del, one allele of *CDKN2A* is deleted, and the other is silenced by DNA methylation. In Hemi-del, *CDKN2A* is suppressed by 2 hits but *CDKN2B* and *MTAP* are not suppressed, due to a single hit. This explains our IHC results (C) and may explain the gradation of poor prognosis in the order of Homo-del, Hemi-del, and Neutral. *CDKN2A/B*, cyclin-dependent kinase inhibitor 2A/B; Hemi-del, hemizygous deletion; Homo-del, homozygous deletion; M, methylated; *MTAP*, methylthioadenosine phosphorylase; Neutral, copy-neutral; U, unmethylated.

malignant transformation which was shortest in Homo-del, and longest in Neutral (Supplementary Figure S4). Although a strong selection bias existed and the sample size was small in this analysis, the results may suggest that the Neutral status is prone to recurrence with good prognosis; and recurrence with poor prognosis is more likely to occur in Hemi-del and Homo-del in astrocytoma. Similarly, we investigated the impact of *CDKN2A/B* status on oligodendroglioma. In some cases, the effect of *CDKN2A/B* status could not be evaluated because they did not reach the OS endpoint for oligodendroglioma. Hemi-del significantly shortened PFS for oligodendroglioma in our cohort (Figure 2B) and tended to have a shorter PFS than Neutral in TCGA-LGG (Figure 2D). Its clinical significance on oligodendroglioma remains unclear and further investigations are warranted.

Hemi-del *CDKN2A/B* may affect prognosis, especially in astrocytoma. Thus, the diagnosis of Hemi-del *CDKN2A/B* is of clinical significance. The present study provides support for the effectiveness of using immunohistochemistry. The Homo-del revealed p16-negative with MTAP loss, while the Hemi-del revealed p16-negative with MTAP retention. In this study, all 16 cases concurred with *CDKN2A/B* status. Immunostaining is undoubtedly useful, and the effectiveness of MTAP immunostaining as a surrogate marker for *CDKN2A/B* status has recently been reported.[47] However, it should be noted that the Hemi-del *CDKN2A/B*, which we insist is meaningful, could not be detected by MTAP immunostaining alone. Moreover, cases with Homo-del *CDKN2A/B* without the loss of MTAP have been reported.[47] The study reported that although *MTAP* is located at a locus adjacent to *CDKN2A*, several cases did not exhibit a clear correlation between *MTAP* and *CDKN2A*. This was confirmed by plotting the copy number correlation between *CDKN2A* and *MTAP* in TCGA-LGG (Supplementary Figure S5). Accordingly, for a more robust assessment of *CDKN2A/B* status, immunohistochemistry combining p16 and MTAP may be superior to MTAP alone. Whereas, when interpreting the results of molecular diagnosis, it is necessary to bear in mind that tumor sampling is affected by dilution when performed at a site with low tumor density. Since the copy number is biased toward neutral due to the contamination of non-tumor-derived DNA, it is necessary to correct the copy number; thus, we determined the tumor content rate by digital PCR. Immunohistochemical analysis, which does not require the use of multiple experiments or calculations to correct for copy numbers, could be a simpler and less expensive alternative. This molecular analysis is a promising method for assessing copy number, especially in settings with limited access to high-throughput sequencing. Furthermore, we believe that immunohistochemical analysis is a promising method to evaluate intra-tumor heterogeneity, especially regarding the extent and rate of *CDKN2A/B* deletion. In one of the Hemi-del cases (case 11), regions exhibiting *CDKN2A/B* Hemi-del and Neutral cells coexisted, demonstrating the heterogeneity of the tumor (Supplementary Figure S3). Heterogeneity within a tumor may be overlooked in bulk molecular analysis, especially when the deletion population is small. Immunohistochemistry enables us to approach the currently unclear issue of whether heterogeneity in tumors containing Homo-del clones exists and whether it affects prognosis.

A crucial finding in this study is the discrepancy in p16/MTAP immunostaining in Hemi-del cases. The *MTAP* locus is located downstream adjacent to the *CDKN2A* locus encoding $p16^{INK4A}$. Deletion of *CDKN2A/B* is accompanied by the deletion of *MTAP* (Supplementary Figure S5), and this reflects the loss of both p16 and MTAP in Homo-del. In contrast, immunostaining revealed the loss of p16 encoded on *CDKN2A* and the retention of MTAP. Epigenetic regulation including promoter methylation may be relevant in this regard. In this study, upstream methylation of *CDKN2A* was confirmed in 8 of the 12 Hemi-del. In the TCGA dataset, methylation was confirmed at sites adjacent to methylation sites observed in our cohort, whereby *CDKN2B* and *MTAP* did not have upstream methylation (Figure 3). Promoter methylation on the remaining allele without deletion may affect the loss of p16 expression in Hemi-del. This may constitute a prognostic factor and discrepancy in p16/MTAP. In Hemi-del, only *CDKN2A* was suppressed by 2 hits, but *CDKN2B* and MTAP were not suppressed, due to a single hit (Figure 3B). This may explain the gradation of poor prognosis in the order of Homo-del, Hemi-del, and Neutral. Hemi-del with promoter methylation may be caused by G-CIMP accompanied by IDH mutation. However, it remains unclear whether the same mechanism works in all Hemi-del cases, and methylation could not be confirmed in at least 4 cases. Apart from methylation, other potential causes for the downregulation of p16 expression include local deletion of the coding region, mutations, or other silencing mechanisms. Further investigations are required to resolve this issue.

It is necessary to investigate whether the *CDKN2A/B* Hemi-del group is a homogeneous or heterogeneous population. Immunohistochemical staining revealed that in all cases, the Hemi-del was p16-negative and exhibited retained MTAP; however, this could have been a coincidence because of the small sample size. Dividing the Hemi-del group into 2 groups based on the presence or absence of *CDKN2A* methylation resulted in survival curves suggesting a difference in prognosis (Supplementary Figure S6). This indicates that it may be necessary to treat Hemi-del with methylation as the *CDKN2A* loss group in the same way as Homo-del. Conversely, despite the methylation status of transcription start sites at 1500, where methylation was observed in MS-MLPA, and with a similar division into 2 groups, the same trend was not observed in the TCGA-LGG cohort (Supplementary Figure S6). Hemi-del group heterogeneity warrants further exploration.

In astrocytoma, the Hemi-del *CDKN2A/B* had a greater impact on the prognosis than grade 2 or 3 according to the WHO 2021 classification (Table 3). In our cohort, the evaluation of histological grade 3 did not predict prognosis, such as a reversal of the risk ratio in grade 2/3. Furthermore, Hemi-del was associated with risks in both our and the TCGA-LGG cohorts. Since prognosis prediction by *CDKN2A/B* status is more impactful than histological findings, we propose that astrocytoma with Hemi-del should be considered as more malignant than copy-neutral (eg, grade 2 astrocytoma with Hemi-del *CDKN2A/B* should be treated as a more severe degree compared to grade 3).

There are several limitations to our study. First, this study was a single-center retrospective study with a small sample size. These results, including multivariate analysis, should be verified with a larger size sample. Of note, similar results have been reported for large-scale public data, and multicenter studies analyzing a larger population may validate our results. In addition, oligodendroglioma requires long-term survival analysis due to the natural history of the disease. The observation period in our study may have been insufficient, and further accumulation of longitudinal data is necessary. Moreover, studies are needed to determine the mechanism by which *CDKN2A/B* Hemi-del worsens prognosis, especially regarding the molecular background that contributes in addition to the single allele deletion.

In conclusion, the Hemi-del *CDKN2A/B* had a negative impact on OS in astrocytoma. Immunohistochemistry of p16/MTAP was useful for detecting Hemi-del or Homo-del, and immunohistochemistry may be combined with molecular diagnostics to validate Hemi-del or Homo-del.

Supplementary material

Supplementary material is available online at *Neuro-Oncology* (https://academic.oup.com/neuro-oncology).

Keywords

CDKN2A/B | hemizygous deletion | IDH-mutant glioma | MTAP | p16

Funding

This work was supported by Japanese Society for the Promotion of Science Grants-in-Aid for Scientific Research (JSPS KAKENHI) Award (Grant No. 20K09392, 20K17972, 21H03044, 22K16690, 23H03021, and 23K08545) and Fukuoka Public Health Promotion Organization Cancer Research Fund.

Acknowledgments

The authors thank Kaori Yasuda, Atsushi Doi, Hiroko Hagiwara, and Cell Innovator Inc. (Fukuoka, Japan) for the useful discussions and advice on in-silico analysis.

Conflict of interest statement

The authors declare that they have no conflict of interest.

Authorship statement

Conceived and designed the study: N.H., R.O., H.Y., M.M., D.K., Y.S., Y.F., A.N., and K.Y.. Acquired funding: N.H., M.M., Y.F., Y.S., and K.Y.. Provided study materials: R.O., H.Y., A.S., N.H., M.M., D.K., R.H., Y.S., Y.F., O.T., T.Y., and K.Y.. Collected the data: R.O., H.Y., and N.N.. Performed statistical analysis: R.O.. First draft of the manuscript: R.O.. All authors reviewed and edited the manuscript and approved the final manuscript.

Affiliations

Department of Neurosurgery,Graduate School of Medical Sciences, Kyushu University, Fukuoka, Japan (R.O., N.H., D.K., R.H., Y.S., Y.F., N.N., A.S., A.N., M.M., K.Y.); Department of Neurosurgery, Oita University Faculty of Medicine, Yufu, Oita, Japan (N.H.); Department of Anatomic Pathology, Graduate School of Medical Sciences, Kyushu University, Fukuoka, Japan (H.Y.); Department of Pathology, Graduate School of Medicine, Dentistry and Pharmaceutical Sciences, Okayama University, Okayama, Japan (H.Y.); Department of Clinical Radiology, Graduate School of Medical Sciences, Kyushu University, Fukuoka, Japan (O.T., T.Y.); Department of Neurosurgery, National Hospital Organization Kyushu Medical Center, Clinical Research Institute, Fukuoka, Japan (M.M.)

References

1. Ostrom QT, Bauchet L, Davis FG, et al. The epidemiology of glioma in adults: A state of the science review. *Neuro Oncol*. 2014;16(7):896–913.
2. Louis DN, Perry A, Reifenberger G, et al. The 2016 World Health Organization classification of tumors of the central nervous system: A summary. *Acta Neuropathol*. 2016;131(6):803–820.
3. Louis DN, Perry A, Wesseling P, et al. The 2021 WHO classification of tumors of the central nervous system: A summary. *Neuro Oncol*. 2021;23(8):1231–1251.
4. Aoki K, Nakamura H, Suzuki H, et al. Prognostic relevance of genetic alterations in diffuse lower-grade gliomas. *Neuro Oncol*. 2018;20(1):66–77.
5. Appay R, Dehais C, Maurage CA, et al; POLA Network. CDKN2A homozygous deletion is a strong adverse prognosis factor in diffuse malignant IDH-mutant gliomas. *Neuro Oncol*. 2019;21(12):1519–1528.
6. Korshunov A, Casalini B, Chavez L, et al. Integrated molecular characterization of IDH-mutant glioblastomas. *Neuropathol Appl Neurobiol*. 2019;45(2):108–118.
7. Reis GF, Pekmezci M, Hansen HM, et al. CDKN2A loss is associated with shortened overall survival in lower-grade (World Health Organization Grades II-III) astrocytomas. *J Neuropathol Exp Neurol*. 2015;74(5):442–452.
8. Roy DM, Walsh LA, Desrichard A, et al. Integrated genomics for pinpointing survival loci within arm-level somatic copy number alterations. *Cancer Cell*. 2016;29(5):737–750.
9. Shirahata M, Ono T, Stichel D, et al. Novel, improved grading system(S) for IDH-mutant astrocytic gliomas. *Acta Neuropathol*. 2018;136(1):153–166.
10. James CD, He J, Collins VP, Allalunis-Turner MJ, Day RS. Localization of chromosome 9p homozygous deletions in glioma cell lines with markers

constituting a continuous linkage group. *Cancer Res.* 1993; 53(16): 3674–3676.
11. Jen J, Harper JW, Bigner SH, et al. Deletion of p16 and p15 genes in brain tumors. *Cancer Res.* 1994;54(24):6353–6358.
12. Olopade OI, Jenkins RB, Ransom DT, et al. Molecular analysis of deletions of the short arm of chromosome 9 in human gliomas. *Cancer Res.* 1992;52(9):2523–2529.
13. Hannon GJ, Beach D. p15INK4B is a potential effector of TGF-beta-induced cell cycle arrest. *Nature.* 1994;371(6494):257–261.
14. Serrano M, Hannon GJ, Beach D. A new regulatory motif in cell-cycle control causing specific inhibition of cyclin D/CDK4. *Nature.* 1993;366(6456):704–707.
15. Sherr CJ. Cancer cell cycles. *Science.* 1996;274(5293):1672–1677.
16. Zhang Y, Xiong Y, Yarbrough WG. ARF promotes MDM2 degradation and stabilizes p53: ARF-INK4a locus deletion impairs both the Rb and p53 tumor suppression pathways. *Cell.* 1998;92(6):725–734.
17. Knudson AG, Jr. Mutation and cancer: Statistical study of retinoblastoma. *Proc Natl Acad Sci U S A.* 1971;68(4):820–823.
18. Alves MKS, Faria MHG, Neves Filho EHC, et al. CDKN2A promoter hypermethylation in astrocytomas is associated with age and sex. *Int J Surg.* 2013;11(7):549–553.
19. Watanabe T, Nakamura M, Yonekawa Y, Kleihues P, Ohgaki H. Promoter hypermethylation and homozygous deletion of the p14ARF and p16INK4a genes in oligodendrogliomas. *Acta Neuropathol.* 2001;101(3):185–189.
20. Yin D, Xie D, Hofmann WK, et al. Methylation, expression, and mutation analysis of the cell cycle control genes in human brain tumors. *Oncogene.* 2002;21(54):8372–8378.
21. Kocakavuk E, Johnson KC, Sabedot TS, et al. Hemizygous CDKN2A deletion confers worse survival outcomes in IDHmut-noncodel gliomas. *Neuro Oncol.* 2023;25(9):1721–1723.
22. Hickman RA, Gedvilaite E, Ptashkin R, et al. CDKN2A/B mutations and allele-specific alterations stratify survival outcomes in IDH-mutant astrocytomas. *Acta Neuropathol.* 2023;146(6):845–847.
23. Bortolotto S, Chiadò-Piat L, Cavalla P, et al. CDKN2A/p16 inactivation in the prognosis of oligodendrogliomas. *Int J Cancer.* 2000;88(4):554–557.
24. Garnier L, Vidal C, Chinot O, et al. Characteristics of anaplastic oligodendrogliomas short-term survivors: A POLA network study. *Oncologist.* 2022;27(5):414–423.
25. Higa N, Akahane T, Yokoyama S, et al. Molecular genetic profile of 300 Japanese patients with diffuse gliomas using a glioma-tailored gene panel. *Neurol Med Chir (Tokyo).* 2022;62(9):391–399.
26. The Cancer Genome Atlas Research Network. Comprehensive, integrative genomic analysis of diffuse lower-grade gliomas. *N Engl J Med.* 2015;372(26):2481–2498.
27. Shibui S, Narita Y, Mizusawa J, et al. Randomized trial of chemoradiotherapy and adjuvant chemotherapy with nimustine (ACNU) versus nimustine plus procarbazine for newly diagnosed anaplastic astrocytoma and glioblastoma (JCOG0305). *Cancer Chemother Pharmacol.* 2013;71(2):511–521.
28. Hata N, Yoshimoto K, Hatae R, et al. Deferred radiotherapy and upfront procarbazine-ACNU-vincristine administration for 1p19q codeleted oligodendroglial tumors are associated with favorable outcome without compromising patient performance, regardless of WHO grade. *Onco Targets Ther.* 2016;9:7123–7131.
29. Kuga D, Hata N, Akagi Y, et al. The effectiveness of salvage treatments for recurrent lesions of oligodendrogliomas previously treated with upfront chemotherapy. *World Neurosurg.* 2018;114:e735–e742.
30. Funakoshi Y, Hata N, Takigawa K, et al. Clinical significance of CDKN2A homozygous deletion in combination with methylated MGMT status for IDH-wildtype glioblastoma. *Cancer Med.* 2021;10(10):3177–3187.
31. Hatae R, Hata N, Yoshimoto K, et al. Precise detection of IDH1/2 and BRAF hotspot mutations in clinical glioma tissues by a differential calculus analysis of high-resolution melting data. *PLoS One.* 2016;11(8):e0160489.
32. Mizoguchi M, Hata N, Kuga D, et al. Clinical implications of molecular analysis in diffuse glioma stratification. *Brain Tumor Pathol.* 2021;38(3):210–217.
33. Simon M, Hosen I, Gousias K, et al. TERT promoter mutations: A novel independent prognostic factor in primary glioblastomas. *Neuro Oncol.* 2015;17(1):45–52.
34. Yoshimoto K, Hatae R, Sangatsuda Y, et al. Prevalence and clinicopathological features of H3.3 G34-mutant high-grade gliomas: A retrospective study of 411 consecutive glioma cases in a single institution. *Brain Tumor Pathol.* 2017;34(3):103–112.
35. Hatae R, Hata N, Suzuki SO, et al. A comprehensive analysis identifies BRAF hotspot mutations associated with gliomas with peculiar epithelial morphology. *Neuropathology.* 2017;37(3):191–199.
36. Araki Y, Mizoguchi M, Yoshimoto K, et al. Quantitative digital assessment of MGMT immunohistochemical expression in glioblastoma tissue. *Brain Tumor Pathol.* 2011;28(1):25–31.
37. Otsuji R, Fujioka Y, Hata N, et al. Liquid biopsy with multiplex ligation-dependent probe amplification targeting cell-free tumor DNA in cerebrospinal fluid from patients with adult diffuse glioma. *Neuro Oncol Adv.* 2022;5(1):vdac178.
38. Hata N, Yoshimoto K, Yokoyama N, et al. Allelic losses of chromosome 10 in glioma tissues detected by quantitative single-strand conformation polymorphism analysis. *Clin Chem.* 2006;52(3):370–378.
39. Mizoguchi M, Kuga D, Guan Y, et al. Loss of heterozygosity analysis in malignant gliomas. *Brain Tumor Pathol.* 2011;28(3):191–196.
40. Mizoguchi M, Yoshimoto K, Ma X, et al. Molecular characteristics of glioblastoma with 1p/19q co-deletion. *Brain Tumor Pathol.* 2012;29(3):148–153.
41. Yoshimoto K, Iwaki T, Inamura T, et al. Multiplexed analysis of post-PCR fluorescence-labeled microsatellite alleles and statistical evaluation of their imbalance in brain tumors. *Jpn J Cancer Res.* 2002;93(3):284–290.
42. Jeuken JWM, Comelissen S, Boots-Sprenger S, Gijsen S, Wesseling P. Multiplex ligation-dependent probe amplification: A diagnostic tool for simultaneous identification of different genetic markers in glial tumors. *J Mol Diagnostics.* 2006;8(4):433–443.
43. Kuo LT, Lu HY, Lee CC, et al. Multiplexed methylation profiles of tumor suppressor genes and clinical outcome in oligodendroglial tumors. *Cancer Med.* 2016;5(8):1830–1839.
44. Fujioka Y, Hata N, Akagi Y, et al. Molecular diagnosis of diffuse glioma using a chip-based digital PCR system to analyze IDH, TERT, and H3 mutations in the cerebrospinal fluid. *J Neurooncol.* 2021;152(1):47–54.
45. Jiromaru R, Yamamoto H, Yasumatsu R, et al. p16 overexpression and Rb loss correlate with high-risk HPV infection in oropharyngeal squamous cell carcinoma. *Histopathology.* 2021;79(3):358–369.
46. Mermel CH, Schumacher SE, Hill B, et al. GISTIC2.0 facilitates sensitive and confident localization of the targets of focal somatic copy-number alteration in human cancers. *Genome Biol.* 2011;12(4):R41.
47. Satomi K, Ohno M, Matsushita Y, et al. Utility of methylthioadenosine phosphorylase immunohistochemical deficiency as a surrogate for CDKN2A homozygous deletion in the assessment of adult-type infiltrating astrocytoma. *Mod Pathol.* 2021;34(4):688–700.